# Multiterminal DC Transmission Systems Based on Superconducting Cables Feasibility Study, Modeling, and Control

Dimitrios I. Doukas, *Member, IEEE*, Argyrios Syrpas, *Student Member, IEEE*, and Dimitris P. Labridis, *Senior Member, IEEE*

***Abstract*—This paper deals with the appropriate modeling and control strategy of a multiterminal dc transmission (MTDC) system that incorporates high-temperature superconducting (HTS) dc cables. The system is based on voltage source converters for the interconnection of stiff ac grids. An overview of the high voltage direct current power transfer technology along with the possibilities it enables, as well as an introduction to the concept of multiterminal topology are presented. The operation principles of the superconducting technology are described and the control strategy of HTS-based MTDC networks is presented. To validate the performance and the dynamic response of the system under steady state as well as under fault and load change conditions, a typical four-terminal MTDC network in ring topology is developed in MATLAB/Simulink.**

***Index Terms*—Droop control, large-scale HTS applications, multi-terminal dc (MTDC) transmission, superconducting transmission, voltage source converter (VSC).**

## I. Introduction

PROGRESS in the technology of superconducting materials by means of modern higher temperature superconductors of lower cost in parallel with the increased power demand, especially within congested urban environments indicate that superconducting components, such as dc cables, can play a significant role [1]. To that end, adoption of superconductors, while taking advantage of the functionalities that state-of-the-art power converters can contribute for dc transmission might lead to HTS-based dc power systems.

A series of attempts can be found in literature, towards this direction, the earliest of which can be found in [2] where the feasibility of high-capacity dc transmission (in the range of GWs) was assessed. At that time, such efforts could be implemented only by cooling with helium, since the material under-study was $Nb_3Sn$ and operation temperatures were lower than 4 K. A few years later, at Los Alamos Scientific Laboratory (LASL), more details were presented, while limitations and advantages of cryogens were pointed out [3]. Adoption of alternative cooling configurations based on liquid hydrogen were first introduced and concerns about security-of-supply were stressed out.

In LASL, more efforts towards the development of superconducting dc cables followed and details about such systems were published in [4], revealing promising results about the applicability of superconducting dc cables and their incorporation within large either ac or dc grids. Most important, some years later, the discovery of high-temperature superconducting materials [5] proved a game-changer opening new perspectives for a series of applications, since a significantly more cost-effective cooling system could be utilized.

In regards to the dc enabling technologies, the development of advanced converter topologies was crucial, while the contribution of voltage-source converters (VSCs) contribution in more efficient, flexible and controllable transmission links proved of critical importance [6]. Moreover, modular multilevel converter topologies, unlocked additional functionalities for high-power applications, a series of which is reviewed in [7], while studies related to pulse width modulation (PWM), control methods and their operation within HVDC systems, under both steady-state and fault conditions came to fruition.

The SuperCity and SuperGrid projects came next as an attempt to combine HTS dc cables and channels of liquid hydrogen [8]–[10]. Special emphasis was given on the development of high-capacity HTS dc systems over long distances and their integration to grid.

In [11], coexistence of HTS dc cables and modular VSCs, within a power system dominated by dc is investigated. Emphasis is given on the voltage level at which the VSC-based dc links operate, which is in the range of 50 kV, in order to take advantage of the high-current low-loss characteristic of HTS transmission links. Apart from reducing transmission losses, stepping down in terms of voltage on the dc side allows for less complex and bulky as well as cheaper converter stations.

More recently, the Electric Power Research Institute (EPRI) presented a significant amount of R&D in the area [12], whereas multi-terminal dc systems based on HTS cables were discussed [13]. More specifically, main focus was given on the power flow and transient stability issues associated with the integration of a HTS dc cables within existing power systems. The important parameters that affect the operation of an HTS-based multi-terminal dc (MTDC) are pointed out, especially related to stability, and a high-level feasibility study is presented. Through

Manuscript received November 28, 2017; accepted February 12, 2018. Date of publication February 14, 2018; date of current version March 6, 2018. *(Corresponding author: Dimitrios I. Doukas.)*

The authors are with the School of Electrical and Computer Engineering, Aristotle University of Thessaloniki, Thessaloniki 54124, Greece (e-mail: doux@auth.gr; syrpas92@gmail.com; labridis@auth.gr).

Color versions of one or more of the figures in this paper are available online at http://ieeexplore.ieee.org.

Digital Object Identifier 10.1109/TASC.2018.2806081

1051-8223 © 2018 EU

these reports, EPRI described the role VSCs could play to the construction and operation of an MTDC power system that is based on HTS links and is able to carry power in the range of 10 GWs.

Finally, in [14], HTS dc cables are presented as a viable alternative to conventional transmission cables, while remarkable advantages in terms of reduced losses (up to 80%) and reduced right of way (up to 85%) can be achieved. An investigation about various grid-integration setups of HTS dc transmission links within ac, dc or mixed ac/dc grids analyzing both steady-state and faults was presented in [15].

The scope of this paper is to address how HTS-based MTDC grids to be modeled and to assess if control techniques applied on conventional MTDC systems, are feasible to be applied on such systems. This paper's contribution is to present detailed modeling and control of a 4-terminal MTDC configuration and to prove that with appropriate treatment of low-damping on control level and by suitable modeling, an MTDC based on HTS cables can be a promising alternative.

In Section II and III, an overview of MTDC advantages, structure and control is presented. In Section IV, details related to the examined case study are illustrated, whereas in Section V, results for different simulation setups are summarized. Section VI presents a discussion on the cable model used as well as on necessary control enhancements that were utilized. Finally, Section VII concludes the paper.

## II. Multi-Terminal DC Systems

MTDC systems have numerous advantages over the point-to-point dc connections due to the reliable and continuous system operation and the power dispatch flexibility [16]. With a MTDC network it is possible to have more than two interconnected ac networks, as well as to link an increased number of remote generation to the main grid [17].

The common practice is the interconnection of each offshore wind-farm with one independent dc transmission line. Consequently, any installation requires the construction of a new dc line. This is considered as an obstacle for new installations, both for financial and environmental reasons. The concept of MTDC networks provides the opportunity to connect any new installation to the nearest existing dc line [18], a feature that reduces the investment and operational costs.

Moreover, in case a problem is encountered, the power is feasible to be transferred via an alternative path, which is not possible in a point-to-point connection that in case of a fault would probably collapse. The MTDC topology enhances the cost-effective interconnection of more generation/demand nodes, making even the creation of a network in the North Sea, to effectively exploit the significant wind energy potential [19], feasible. Such a system could be combined with HTS cables, leading to applications with even lower losses and more techno-economic advantages [15], [20].

## III. Basic Control Techniques

In a multi-terminal HVDC network under normal conditions, the dc voltage should be maintained within a limited range at a specific value, which is in most cases the nominal. A larger voltage deviation would lead to the activation of protective devices or even to a possible collapse of the network. A constant value of the dc voltage with a limited accepted ripple indicates that the power balance between the terminals has been achieved [21].

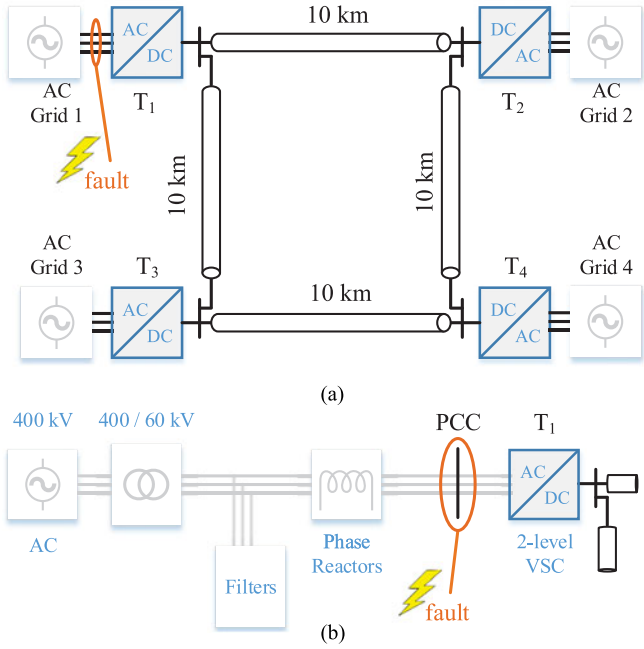


Fig. 1. Configuration of a four-terminal VSC-MTDC grid. (a) High-level representation of a four-terminal MTDC grid. (b) Detailed representation of Area 1 and fault allocation.

Several control approaches can be found in literature [22], [23], indicating that the dc voltage should be allocated to more than one converter stations. The most widely used technique to achieve this distributed control is droop control, which allows all converters to participate to the regulation of active power based on their dc voltage deviations [24]. If the voltage of the terminal increases, this means that there is a surplus of active power in the grid, so the converter has to increase its active power output, to inject more power to the ac side. This is achieved through linear correlation between the active power and the terminal dc voltage. The similar occurs, if the power flow of the network is decreased:

$$\Delta P = \frac{1}{k}\Delta v \tag{1}$$

where $k$ is the droop gain and $\Delta P$, $\Delta v$ are the deviations of active power and dc voltage, respectively. $\Delta P$ is related to $\Delta v$. The reference power $P_{\mathrm{ref}}$ is the sum of the initial reference power $P_{\mathrm{ref,in}}$ and $\Delta P$ and is subtracted from the measured power $P_{\mathrm{meas}}$ and then passes through a PI controller, to result as the reference of the current in the $d$ axis.

## IV. Modeling & Control - Case Study

To study an HTS-based MTDC system, the four-terminal system of Fig. 1(a) is examined. All four areas of the Fig. 1(b)

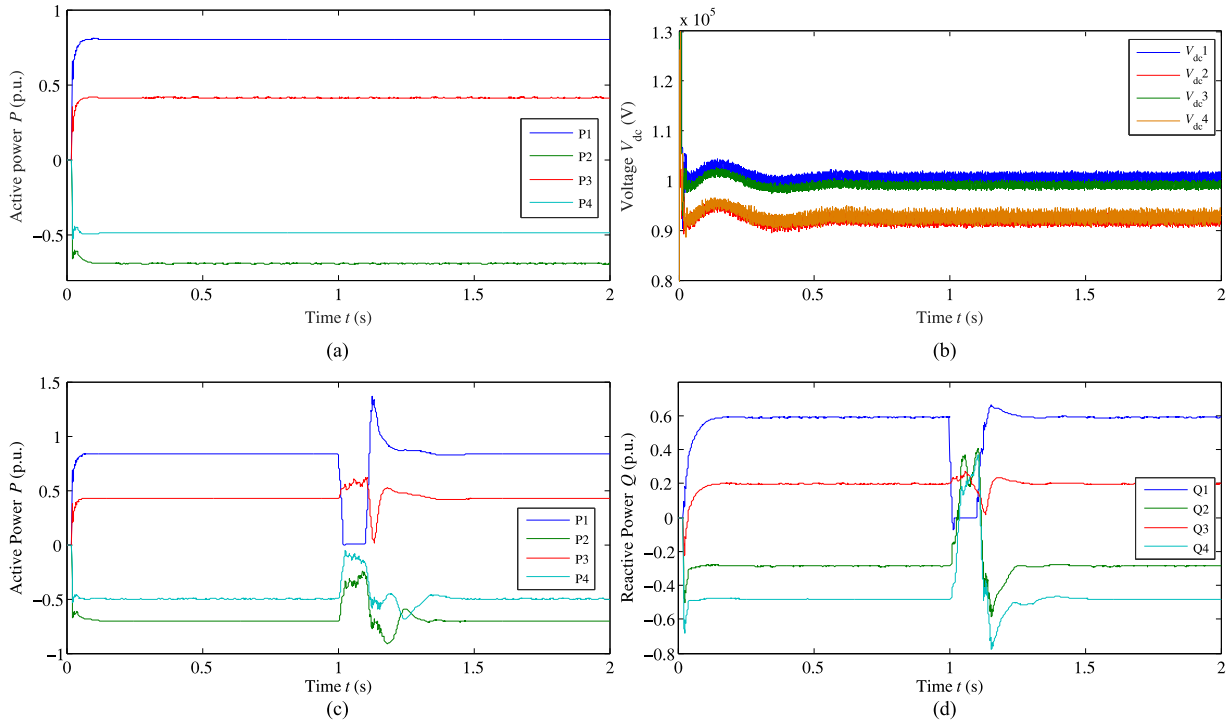


Fig. 2. Summarized results for steady state and fault scenarios in case of HTS cables integration. (a) Steady-state scenario: active power flow. (b) Steady-state scenario: dc voltage. (c) Fault scenario: active power flow. (d) Fault scenario: reactive power flow.

are identical with each other and an example in more detail can be seen in Fig. 1(b).

For the HTS cables the distributed parameters model is used and the configuration is the one of [12]. The same cross-section is used also for the conventional dc cable, but copper is considered instead. Regarding the cable integration, for each link two cables are used one of which is connected to the ground while high voltage is applied to the second.

Filters and phase reactors are included on the ac side, whereas smoothing inductors, capacitors and filters are incorporated on the dc side, as seen in Fig. 1(b). Regarding the converter topology, a 2-level VSC is used in all converters' stations allowing bi-directional active and reactive power flow across the whole MTDC system. PWM at carrier signal frequency of 4050 Hz is used after taking into account that higher frequencies would result in more high-quality signals but on increased switching losses as well.

The Terminals ($T_1$–$T_4$) operate independently and each Terminal is able to control two physical quantities, which are determined by the nature of the interconnected networks. In this case, the Terminals connect four stiff ac networks and each Terminal applies the same droop control method. Control for the active and the reactive power was based on (2)–(3)

$$P = \frac{V_{\rm ac} V_{\rm conv} \sin\delta}{X_s} \tag{2}$$

$$Q = \frac{V_{\rm ac} V_{\rm conv} \cos\delta}{X_s} - \frac{V_{\rm conv}^2}{X_s} \tag{3}$$

Cascade control using PI controllers for fast system response is used. This is implemented by two control loops in series, while the external loop is the input for the inner one. The inner loop is responsible for the control of the most rapidly changing parameter, such as current, while the exterior loop controls other physical parameters, such as active power.

### A. Test Cases

Initially a steady state scenario is simulated and then the dynamic behavior of the system was tested in case of power flow changes and faults. Our power base reference is set at 500 MVA. The reference conditions were defined as follows:

- $T_1$ injects to the grid 0.8 p.u. $P$ and 0.6 p.u. $Q$.
- $T_2$ absorbs from the grid 0.7 p.u. $P$ and 0.3 p.u. $Q$.
- $T_3$ injects to the grid 0.4 p.u. $P$ and 0.2 p.u. $Q$.
- $T_4$ absorbs from the grid 0.5 p.u. $P$ and $Q$.

All ac grids operate at 400 kV and transformers are used to step down the voltage at 60 kV. The dc voltage is then converted to 100 kV.

A fault scenario, more specifically a three-phase short-circuit, that occurs at 1.0 s and lasts 0.1 s, i.e., until 1.1 s is also studied in order for the MTDC system response to be examined. The normal operation is restored at 1.1 s. The fault takes place at the point of common coupling (PCC) of the ac network 1 with the terminal $T_1$, as seen in Fig. 1(a) and in more detail in Fig. 1(b).

## V. Results

Results considering both examined scenarios are summarized in Fig. 2. For brevity results regarding total harmonic distortion (THD) are not included, but THD of voltage and current on dc side equals 1.16% and 2.34%, respectively.

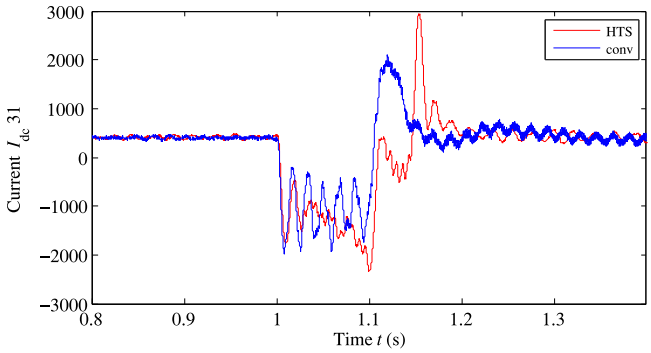


Fig. 3. Current $I_{\mathrm{dc}}31$ in case of HTS and conventional cable.

In Fig. 2(a) and (b), active power flow and voltages on dc side for the steady-state scenario are presented. The voltage drop is larger at the $\mathrm{T}_2$ and $\mathrm{T}_4$, compared to $\mathrm{T}_1$ and $\mathrm{T}_3$, due to the fact that the first two terminals absorb power from the grid, whereas the last two inject. In Fig. 2(c) and (d), results for the fault scenario are illustrated. It is evident that $\mathrm{T}_1$ and $\mathrm{T}_3$ that inject power experience greater disturbances and fluctuations in their active power outputs than in their reactive, whereas for the receiving stations, $\mathrm{T}_2$ and $\mathrm{T}_4$, the opposite occurs.

The same fault scenario is simulated in case of a conventional cable to compare their transient response. For brevity, results only for current $I_{\mathrm{dc},31}$, which is the dc current that flows through the cable that connects terminals $\mathrm{T}_1$ and $\mathrm{T}_3$, is presented in Fig. 3. Focus is given on this link, since it is in close proximity with the fault position, i.e., it is more affected.

According to Fig. 3, in case of the HTS cable, the peak over-current during post-fault period reaches 3 kA, i.e., 1 kA more than in the case a conventional cable was used for the same link. Moreover, as expected, the damping in case of the conventional cable is better during the post-fault period when compared with the HTS scenario. Oscillations are more persisting in case of the HTS connection due to the significantly lower series resistance. In this work, the critical current above which the HTS equipment is led to quenching is considered equal to 6.5 kA, therefore no quenching can be assumed for both cases. However, in case of longer or most severe faults, the over-currents during the post-fault period could be more significant.

## VI. Discussion

A brief discussion on cable modeling and the control approach utilized is needed. Firstly, in regards to the cable model for transient studies, the importance of the transmission length needs to be pointed out, since it affects the dominant transient frequency of the cable [25]. Secondly, to work with a purely electrical cable model, such as the one proposed by EPRI in Fig. 4, the dc resistivity of both HTS layers is taken equal to $10^{-12}\ \Omega$ m, while the respective resistivity of the metallic sheath equals $3 \cdot 10^{-8}\ \Omega$ m. Moreover, $\epsilon_r$ and $\mu_r$ that refer to the insulators' relative electrical permittivity and magnetic permeability, are considered equal to 2.5 and 1.0, respectively [12].

The dominant frequency, at which per-unit length impedance $\mathbf{Z}$ and admittance $\mathbf{Y}$ matrices were calculated is equal to

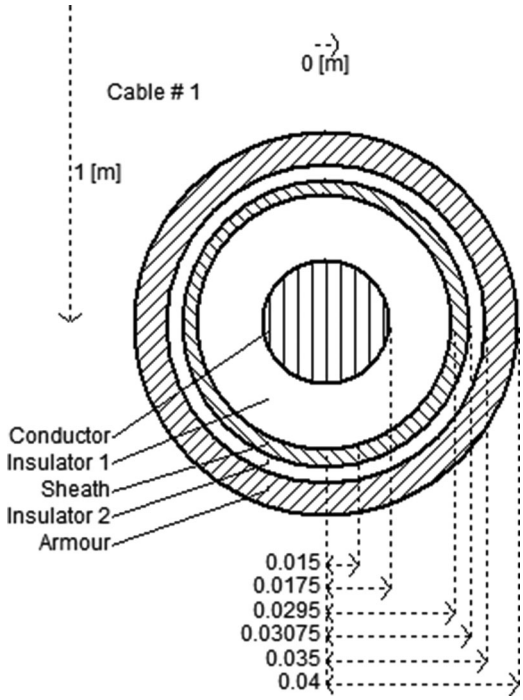


Fig. 4. Cable arrangement geometry characteristics.

4.7 kHz, while for the calculation ATP has been utilized. PSCAD/EMTDC has been used for validation, resulting in identical results with ATP. Influence of the difference between room and cryogenic temperature to the resistivity was not considered.

These matrices are then used as input to the distributed parameter model that MATLAB/Simulink includes. Cable parameters calculation at a single frequency was necessary since system modeling has been done with MATLAB/Simulink and its cable model is based on the electrical parameters calculated at one frequency, which here is the dominant, since transients are studied as well. Unlike conventional cables, single frequency calculations do not constitute modeling limitation in case of HTS cables, because the latter present the same impedance over all frequencies [12].

In most studies, when an HTS cable is considered with the Π-equivalent model, the series resistance is considered several times of magnitude lower than the corresponding resistance of conventional materials, such as copper or aluminum. However, with the distributed parameters modeling, which is examined here, and given that the outer metallic sheath is made of steel and is considered grounded, the earth effect on the $\mathbf{Z}$ matrix is significant and the matrix values for the HTS cable are marginally smaller than the ones of the same cable made by copper. Note, that the elements of the matrices in (4) and (5) would be indeed significantly different in case the cable armor was also made of a superconducting material and in case the earth's resistivity was also considered ≈0.

In the matrices (4) and (5), the per unit length resistance matrix $\mathbf{R}$, assuming either a superconductor ($\rho = 10^{-12}\ \Omega$m) or copper ($\rho = 3 \cdot 10^{-8}\ \Omega$m), is presented and it is evident that the difference on the matrices values is insignificant. This does not

mean that losses under steady-state conditions are similar, since as seen in [15] losses are indeed minimized when HTS cables are utilized. However, in case of transients, this small deviation of the matrices' elements leads to comparable transient responses. Note, that the resistance values that are included in (4) and (5) are not the ones used for power flow and control, otherwise the slight difference between the HTS and the copper case would result in similar transmission losses. Moreover, the calculated matrices' elements refer only to the cable component and are independent from the examined simulation and depend only on the geometry, the material properties, the frequency and the surrounding conditions.

$$\mathbf{R}_{\mathrm{HTS}} = \begin{bmatrix} 4.7982 \cdot 10^{-3} & 4.7981 \cdot 10^{-3} & 4.6867 \cdot 10^{-3} \\ 4.7981 \cdot 10^{-3} & 4.7981 \cdot 10^{-3} & 4.6867 \cdot 10^{-3} \\ 4.6867 \cdot 10^{-3} & 4.6867 \cdot 10^{-3} & 4.6813 \cdot 10^{-3} \end{bmatrix} \times (\Omega/\mathrm{m}) \tag{4}$$

$$\mathbf{R}_{\mathrm{Cu}} = \begin{bmatrix} 5.0490 \cdot 10^{-3} & 4.8175 \cdot 10^{-3} & 4.6869 \cdot 10^{-3} \\ 4.8175 \cdot 10^{-3} & 4.9353 \cdot 10^{-3} & 4.6869 \cdot 10^{-3} \\ 4.6869 \cdot 10^{-3} & 4.6869 \cdot 10^{-3} & 4.6815 \cdot 10^{-3} \end{bmatrix} \times (\Omega/\mathrm{m}) \tag{5}$$

Focus is given on how different resistivity values are translated to different resistance $\mathbf{R}$ matrices. The corresponding $\mathbf{L}$ and $\mathbf{C}$ matrices, for inductance and capacitance respectively, have identical numbers with each other and are not presented. That occurs because of the same cable geometry and because operation in dc leads to no skin effect considerations. These similarities regarding the $\mathbf{R}$ matrices for both the HTS and copper cases can be generalized in case a different cross-section was under study. Cable modeling limitations may exist in case of faults or conditions that lead us to over-currents outside the critical current, since the transition from the superconducting to the resistive state due to high ampacity, i.e., quenching, may not be represented adequately without coupled electro-thermal model of the cable [26], [27]. However, critical currents can reach 7-10 kA [28] and since in this study, fault currents will not exceed these values, no quenching can be assumed.

Moreover, improvements on the control level are necessary in case of HTS dc transmission to provide additional damping.

• Current Limiter. In case of faults or transients, current fed into the reactor needs to be limited. The current limiter is implemented in order to protect from disturbances in the outer controllers. Depending on the operation mode, active or reactive power might be of greater significance. In this paper, priority is given to active power ($d$ axis current component) and $i^{d\mathrm{ref}}$ is compared to $I_{\max}$. If $i^{d\mathrm{ref}}$ is still greater, then it is saturated to $I_{\max}$ and $i^{q\mathrm{ref}}$ is zero. Else if it is smaller, then $i^{d\mathrm{ref}}$ is processed unchanged to the output and $i^{q\mathrm{ref}}$ becomes $i^{q\mathrm{ref}} = \sqrt{I_{\max}^2 - (i^{d\mathrm{ref}})^2}$. Thus, the ac inductors are protected from overheating in case of current inrush, the HTS transmission line is protected from quenching and the two grids become de-coupled in terms of fault propagation.

• Integral wind-up refers to the situation where a large change in set-point occurs and the integral term of the PI keeps accumulating a significant control error during the rise (windup), resulting to overshooting and continuing to increase as the accumulated error is unwound. In this paper, this is treated by the method of back-calculation. When the output saturates, the integral term in the controller is recomputed with the aid of a feedback term so that its new value gives an output at the saturation limit [29].

## VII. Conclusion

Feasible modeling of a four-terminal MTDC network utilizing HTS cables to interconnect stiff ac systems is developed and presented. Feasibility study of control techniques applied on conventional MTDC systems are also presented and discussed. Steady-state operation, power flow changes as well as faults are studied. Modeling approaches are not implying themselves better results, however indications on how more efficient control is to be structured are stated. A thorough discussion regarding the HTS cable model that was used in this work and a detailed comparison between conventional cables are presented. It is observed that by the proposed control approach, the system, despite its low-damping characteristic, presents a well-damped behavior.

The proposed structure indicates that HTS-based MTDC grids are technically feasible. Transition to MTDC grids that incorporate coupled electro-thermal cable models will be the focus of our future research.

## Acknowledgment

The authors would like to thank Mrs. Z. D. Blatsi, power electronics engineer at TE/EPC of CERN, for useful advice on control as well as on the latest HTS application developments.

## References

[1] D. I. Doukas, Z. D. Blatsi, A. N. Milioudis, D. P. Labridis, L. Harnefors, and G. Velotto, "Damping of electromagnetic transients in a superconducting VSC transmission system," in *Proc. 2015 IEEE Eindhoven PowerTech*, Jun. 2015, pp. 1–6.

[2] R. L. Garwin and J. Matisoo, "Superconducting lines for the transmission of large amounts of electrical power over great distances," *Proc. IEEE*, vol. 55, no. 4, pp. 538–548, Apr. 1967.

[3] J. R. Bartlit, F. J. Edeskuty, and E. F. Hammel, "The supercable: Dual delivery of hydrogen and electric power," in *Proc. 4th Int. Conf. 1972 Cryogenic Eng.*, May 1972, pp. 177–180.

[4] F. J. Edeskuty, "The DC superconducting power transmission line project at LASL: US DOE division of electric energy systems," Tech. Rep. 54-86, LA-08323-PR, Apr. 1980.

[5] J. G. Bednorz and K. A. Müller, "Possible high Tc superconductivity in the Ba-La-Cu-O system," *Zeitschrift für Physik B: Condensed Matter*, vol. 64, pp. 189–193, Apr. 1986.

[6] N. Flourentzou, V. G. Agelidis, and G. D. Demetriades, "VSC-based HVDC power transmission systems: An overview," *IEEE Trans. Power Electron.*, vol. 24, no. 3, pp. 592–602, Mar. 2009.

[7] A. Nami, J. Liang, F. Dijkhuizen, and G. D. Demetriades, "Modular multilevel converters for HVDC applications: Review on converter cells and functionalities," *IEEE Trans. Power Electron.*, vol. 30, no. 1, pp. 18–36, Jan. 2015.

[8] P. M. Grant, "Energy for the city of the future," *Ind. Physicist*, vol. 8, no. 1, pp. 22–25, 2002.

[9] C. Starr, "National energy planning for the century," in *Proc. Amer. Nucl. Soc. Winter Meeting, Reno, NV, USA*, 2001, pp. 31–35.

[10] C. Starr, "National energy planning for the century: The continental SuperGrid," *Semicond.*, vol. 16, 2002, Art. no. 17.
[11] G. Venkataramanan and B. K. Johnson, "A superconducting DC transmission system based on VSC transmission technologies," *IEEE Trans. Appl. Supercond.*, vol. 13, no. 2, pp. 1922–1925, Jun. 2003.
[12] "Program on technology innovation: Transient response of a superconducting DC long length cable system using voltage source converters," *Elect. Power Res. Inst.*, Palo Alto, CA, USA, Tech. Rep. 1020339, Dec. 2009.
[13] "Program on technology innovation: Study on the integration of high temperature superconducting DC cables within the eastern and western north American power grids," Elect. Power Res. Inst., Palo Alto, CA, USA, Tech. Rep. 1020330, Nov. 2009.
[14] A. Morandi, "HTS DC transmission and distribution: concepts, applications and benefits," *Supercond. Sci. Technol.*, vol. 28, no. 12, Oct. 2015, Art. no. 123001.
[15] D. I. Doukas, Z. D. Blatsi, and D. P. Labridis, "Grid integration scenarios for superconducting DC transmission systems," in *Proc. 2017 IEEE Manchester PowerTech*, Jun. 2017, pp. 1–6.
[16] G. Stamatiou and M. Bongiorno, "Power-dependent droop-based control strategy for multi-terminal HVDC transmission grids," *IET Gener. Transmiss. Distrib.*, vol. 11, no. 2, pp. 383–391, Jan. 2017.
[17] J. Wu, S. Zhang, and D. Xu, "Modeling and control of multi-terminal HVDC with offshore wind farm integration and DC chopper based protection strategies," in *Proc. 2013–39th Annu. Conf. IEEE Ind. Electron. Soc.*, Nov. 2013, pp. 1013–1018.
[18] X. Zhao, Q. Song, H. Rao, X. Li, X. Li, and W. Liu, "Control of multi-terminal VSC-HVDC system to integrate large offshore wind farms," *Int. J. Comput. Elect. Eng.*, vol. 5, no. 2, pp. 201–206, Apr. 2013.
[19] E. J. Wiggelinkhuizen, J. T. G. Pierik, and R. T. Pinto, "North sea transnational grid, dynamic wind farm model for simulating multi-terminal HVDC grids," ECN, Petten, The Netherlands, Tech. Rep. ECN-E14-006, Feb. 2014.
[20] B. K. Johnson *et al.*, "Superconducting low voltage DC transmission networks," *Elect. Mach. Power Syst.*, vol. 22, no. 6, pp. 629–645, Nov. 1994.
[21] C. E. Spallarossa, T. C. Green, C. Lin, and X. Wu, "A DC voltage control strategy for MMC MTDC grids incorporating multiple master stations," in *Proc. 2014 IEEE PES T&D Conf. Expo.*, Apr. 2014, pp. 1–5.
[22] N. R. Chaudhuri and B. Chaudhuri, "Adaptive droop control for effective power sharing in multi-terminal DC (MTDC) grids," in *2013 Proc. IEEE Power Energy Soc. Gen. Meeting*, Jul. 2013, pp. 21–29.
[23] H. Rao, "Architecture of Nan'ao multi-terminal VSC-HVDC system and its multi-functional control," *CSEE J. Power Energy Syst.*, vol. 1, no. 1, pp. 9–18, Mar. 2015.
[24] W. Wang, M. Barnes, and O. Marjanovic, "Droop control modelling and analysis of multi-terminal VSC-HVDC for offshore wind farms," in *Proc. 10th IET Int. Conf. AC DC Power Transmiss.*, Dec. 2012, pp. 1–6.
[25] A. Ametani and T. Kawamura, "A method of a lightning surge analysis recommended in Japan using EMTP," *IEEE Trans. Power Del.*, vol. 20, no. 2, pp. 867–875, Apr. 2005.
[26] L. Bottura, C. Rosso, and M. Breschi, "A general model for thermal, hydraulic and electric analysis of superconducting cables," *Cryogenics*, vol. 40, no. 8–10, pp. 617–626, Aug. 2000.
[27] D. I. Doukas, A. I. Chrysochos, T. A. Papadopoulos, D. P. Labridis, L. Harnefors, and G. Velotto, "Coupled electro-thermal transient analysis of superconducting dc transmission systems using FDTD and VEM modeling," *IEEE Trans. Appl. Supercond.*, vol. 27, no. 8, Dec. 2017, Art. no. 5401608.
[28] O. Maruyama *et al.*, "Results of Japan's first in-grid operation of 200-MVA superconducting cable system," *IEEE Trans. Appl. Supercond.*, vol. 25, no. 3, Jun. 2015, Art. no. 5401606.
[29] K. J. Åström and R. M. Murray, *Feedback Systems*. Princeton, NJ, USA: Princteton Univ. Press, 2002.